scientific reports

Check for updates

OPEN

Medium optimization to improve growth and iron uptake by *Bacillus tequilensis* ASFS1 using fractional factorial designs

Naghmeh Satarzadeh[1,4], Bagher Amirheidari[1,2]✉, Mojtaba Shakibaie[1,3]✉ & Hamid Forootanfar[1,3]

Many notable applications have been described for magnetic nanoparticles in delivery of diverse drugs and bioactive compounds into cells, magnetofection for the treatment of cancer, photodynamic therapy, photothermal therapy, and magnetic particle imaging (MPI). In response to the growing demand for magnetic nanoparticles for drug delivery or biomedical imaging applications, more effective and eco-friendly methodologies are required for large-scale biosynthesis of this nanoparticles. The major challenge in the large-scale biomedical application of magnetic nanoparticles lies in its low efficiency and optimization of nanoparticle production can address this issue. In the current study, a prediction model is suggested by the fractional factorial designs. The present study aims to optimize culture media components for improved growth and iron uptake of this strain. The result of optimization for iron uptake by the strain ASFS1 is to increase the production of magnetic nanoparticles by this strain for biomedical applications in the future. In the present study, design of experiment method was used to probe the effects of some key medium components (yeast extract, tryptone, $FeSO_4$, Na_2-EDTA, and $FeCl_3$) on Fe content in biomass and dried biomass of strain ASFS1. A 2^{5-1} fractional factorial design showed that Na_2-EDTA, $FeCl_3$, yeast extract-tryptone interaction, and $FeSO_4$-Na_2-EDTA interaction were the most parameters on Fe content in biomass within the experimented levels ($p < 0.05$), while yeast extract, $FeCl_3$, and yeast extract-tryptone interaction were the most significant factors within the experimented levels ($p < 0.05$) to effect on dried biomass of strain ASFS1. The optimum culture media components for the magnetic nanoparticles production by strain ASFS1 was reported to be 7.95 g L^{-1} of yeast extract, 5 g L^{-1} of tryptone, 75 µg mL^{-1} of $FeSO_4$, 192.3 µg mL^{-1} of Na_2-EDTA and 150 µg mL^{-1} of $FeCl_3$ which was theoretically able to produce Fe content in biomass (158 µg mL^{-1}) and dried biomass (2.59 mg mL^{-1}) based on the obtained for medium optimization. Using these culture media components an experimental maximum Fe content in biomass (139 ± 13 µg mL^{-1}) and dried biomass (2.2 ± 0.2 mg mL^{-1}) was obtained, confirming the efficiency of the used method.

Keywords Magnetic iron nanoparticles, Magnetotactic bacteria, *Bacillus tequilensis*, Medium optimization, Fractional factorial designs, Bacterial uptake iron, Prediction model

Nanotechnology is an interdisciplinary field at the forefront of scientific research, encompassing chemistry, fundamental physics, biology, medicine, and material science[1–3]. The concept of nanoscience was first presented by Nobel prize-winning physicist Richard Feynman to construct different materials at the nanoscale level in 1959[3,4]. Nanomaterials comprise various categories of materials if those have at least one dimension smaller than 100 nm[3–5]. Among them, magnetic nanoparticles (MNPs) are an intriguing group of nanoparticles that have been considerably utilized in diverse fields because of their magnetic properties such as targeted drug delivery, sensing technologies, magnetic labeling, engineering, magnetic separation, and environment applications[6–12]. Among

[1]Department of Pharmaceutical Biotechnology, Faculty of Pharmacy, Kerman University of Medical Sciences, Kerman, Iran. [2]Extremophile and Productive Microorganisms Research Center, Kerman University of Medical Sciences, Kerman, Iran. [3]Pharmaceutical Sciences and Cosmetic Products Research Center, Kerman University of Medical Sciences, Kerman, Iran. [4]Stem Cells and Regenerative Medicine Innovation Center, Kerman University of Medical Sciences, Kerman, Iran. ✉email: bah.articles@gmail.com; b_amirheidari@kmu.ac.ir; Shakiba@kmu.ac.ir

MNPs, iron oxide nanoparticles (IONPs) are promising nanoparticles due to their superior biocompatibility for biomedical applications such as magnetic hyperthermia[6,13,14]. The comprehensive investigation efforts are underway to commercialize IONPs for progressive biomedical applications[15]. The superparamagnetic magnetite (Fe_3O_4) is the most common iron oxide compared to α-Fe_2O_3 (hematite) and γ-Fe_2O_3 (maghemite) due to its superior magnetic properties, higher biocompatibility, and lower cytotoxicity[6,16]. Several techniques for preparing nanoparticles have been described, including physical, chemical, and biological methods[3]. The biological synthesis of nanoparticles is being performed by various macro and microscopic organisms such as bacteria, fungi, viruses, yeast, and plant extracts[3,17]. The biosynthesis of nanoparticles has received considerable attention in recent years due to their environment-friendly behavior, lower toxicity, more biocompatibility, and more potential for pharmaceutical and biomedical applications than conventional synthesis including chemical and physical methods[18,19]. Biogenic nanoparticles are remarkably stable and can be made mono-dispersed by changing various factors such as temperature, shaking speed, pH, and incubation duration[20]. Furthermore, magnetic nanoparticles synthesized by biological methods are pharmacologically better than those produced with physical or chemical techniques[21]. However, microbial-assisted Synthesis is slow and needs long stages such as culturing, nanoparticle extraction, and purification[20]. The efficacy of biosynthesis techniques is yet limited to the laboratory step because biosynthesis methods are not still capable of producing large-scale homogeneous nanoparticles[19]. Thus, there is a critical necessity for stable, efficient, scalable, and eco-friendly fabrication procedures[19]. Although there have been significant advancements in the fabrication of nanoparticles using various methods such as hydrothermal reactions, laser pyrolysis, co-precipitation, sol–gel method, electrochemistry, flow injection syntheses, as summarized by Laurent et al[13]. developing an ideal synthetic method for IONP still poses a challenge. This optimal synthesis should meet certain criteria, such as high production yield and avoiding the use of harmful chemicals[22]. Design of experiments (DoE) is described as a mathematical model that can be employed to design and investigate experiments[23]. In addition, this method significantly reduces the number of experiments required to screen a large number of variables (more than three variables) simultaneously[24]. In a DoE experiment, the various factors are discretized into a collection of values that are presented as levels. These levels experiment in various assortments, and a model predicting the response of the system is created based on input data and data collected via multiple iterations of investigation[25]. Fractional Factorial Design (FFD) supplies details on potential high-order interactions, something that is difficult utilizing a full factorial approach – measuring one factor at a time[24]. Another advantage of FFD over full factorial is fewer experimental runs due to decreasing the time needed to obtain data and reducing experiment costs[24,26]. In this study, we carried on our previous microbial synthesis approach using the thermophilic strain ASFS1, producing intracellular superparamagnetic Fe_3O_4 nanoparticles. Utilizing fractional factorial design (FFD), as a collection of mathematical and statistical techniques, we determined the optimal medium composition and ideal productive conditions for cultivating the strain ASFS. Additionally, we employed the dry weight of biomass and iron in the cell plate to monitor the corresponding biomineralization process.

Material and method

Materials and reagents

Tryptone, ferrous sulfate ($FeSO_4$), yeast extract, NaCl, ethylenediaminetetraacetic acid (EDTA), and ferric chloride ($FeCl_3$) were provided by Merck Chemicals (Darmstadt, Germany).

Bacterial strain

Bacillus tequilensis strain ASFS1 (GenBank accession number is MZ669973.1), which magnetic behavior and synthesis of superparamagnetic Fe_3O_4 nanoparticles had proven by Satarzadeh et al[27]. in 2024. This strain was used in this study to optimize the growth of bacteria and the iron uptake.

Biosynthesis of superparamagnetic Fe_3O_4 nanoparticles

To produce magnetite nanoparticles by strain ASFS1, 2 mL of fresh inoculum (equal to 0.5 McFarland) was added to 500 mL Erlenmeyer flasks containing 200 mL of Luria–Bertani medium (containing yeast extract 0.5 g, tryptone 1 g, and NaCl 1 g in 100 ml distilled water) supplemented with $FeSO_4$ (200 µg mL^{-1}) and $FeCl_3$ (400 µg mL^{-1}) and incubated at 37 °C and shaken for 72 h (120 rpm) and then 24 h not shaken according to previous report. After incubation, the bacterial cells were removed from the culture medium by centrifugation (12,800 g for 5 min). The cell pellets were transmitted to a mortar and disrupted by freeze–thaw cycles (5 cycles). Magnetic nanoparticles were separated using a magnetic and reproducible method previously described. In summary, magnetite nanoparticles were separated from disrupted cells using passing via a magnetic separation with a syringe placed near a neodymium-iron-boron magnet and set on solid phase extraction (SPE) Manifolds. Subsequently, the syringe was washed with 1.5 M Tris/HCl buffer (pH 8.3), 1% SDS, and deionized water respectively. Finally, the magnet was separated from the syringe to elute magnetite nanoparticles with deionized water. The obtained magnetite nanoparticles were studied by field-emission scanning electron microscopy (FESEM, Sigma VP model, ZEISS, Germany). This study was conducted to optimize the components of the culture medium to increase the number of cells and subsequently increase the amount of magnetite nanoparticles. The amount of magnetite nanoparticles was analyzed using an indirect method as previously described[28]. In summary, one ml aliquots (96 h incubated) were centrifuged (9600 g for 5 min) and the supernatant was discarded. The cell pellets were washed with sterile 0.9% NaCl solution mixed with 69% nitric acid (1 ml) and incubated at 98 °C for 2 h. The amount of iron in the cell pellets were measured using an atomic absorption spectrometer (AA670, Shimadzu, Japan). To measure the biomass dry weight, one ml of the samples was centrifuged and then dried and weighed.

Experimental design

A 2^{5-1} FFD, was employed to screen the most effective variables in superparamagnetic Fe_3O_4 nanoparticles production by strain ASFS1 and for developed a model for optimal conditions. Luria–Bertani medium was used as the basal medium, and then $FeSO_4$, $FeCl_3$, and ethylenediaminetetraacetate disodium salt dihydrate (Na_2-EDTA) were added to the basal media. The parameters were selected yeast amount (X_1), tryptone amount (X_2), $FeSO_4$ concentration (X_3), Na_2-EDTA concentration (X_4), and $FeCl_3$ concentration (X_5). The range and the levels of the factors showed in Table 1.

A 2^{5-1} FFD with three center points consisting of 19 factorial runs were designed by Design Expert version 6.0.4 statistical software (Table 2). The coding of the factors was accomplished according to the following equation:

$$x_i = \frac{X_i - X_{i;0}}{\Delta X} i = 1,2,3,\ldots,k \quad (1)$$

In this study, x_i refers to the coded value of an independent variable, X_i represents the real value of the independent variable, $X_{i;0}$ denotes the real value of the independent variable at the center point, and ΔX_i represents the step change value. The dry weight of biomass (one ml of bacterial culture) and iron content in biomass (one ml of bacterial culture) were measured as the dependent variable or response. The runs were conducted randomly in an attempt to minimize the influence of extraneous variables. The selected factors can be linked to the response through a model, which is presented in the following equation:

$$Y = b_0 + \sum_{i=1}^{n} b_i x_i + \sum_{i=1}^{n} b_{ii} x_i^2 + \sum_{i=1}^{n-1} \sum_{j=i+1}^{n} b_{ij} x_i x_i + e \quad (2)$$

In this equation, x_i ($i = 1$–5) represents the variables of the experiment. Y denotes the response function, which in this study is Fe content in biomass (Response 1) and dried biomass (Response 2). The variable e represents the

Variable	Component	Unit	Low level (−1)	High level (+1)
X_1	Yeast extract	g L^{-1}	2	8
X_2	Tryptone	g L^{-1}	5	15
X_3	$FeSO_4$	µg mL^{-1}	25	75
X_4	Na_2-EDTA	µg mL^{-1}	0	200
X_5	$FeCl_3$	µg mL^{-1}	50	150

Table1. Utilized Variables for the experimental domain.

	Coded levels					Response 1		Response 2	
						Fe content in biomass (µg mL^{-1})		Dried biomass (mg mL^{-1})	
Run	X_1	X_2	X_3	X_4	X_5	Experimental	Predicted	Experimental	Predicted
1	−1	−1	−1	−1	+1	96.9	89.5	1.2	1.5
2	+1	−1	−1	−1	−1	71.5	69.3	2.3	2.05
3	−1	+1	−1	−1	-1	60.7	49.7	1.4	1.65
4	+1	+1	−1	−1	+1	65.5	86.6	3.3	2.5
5	−1	−1	+1	−1	−1	44.3	34.08	1	0.98
6	+1	−1	+1	−1	+1	122.9	114.3	2.4	2.6
7	−1	+1	+1	−1	+1	79	94.7	2	2.2
8	+1	+1	+1	−1	−1	27.9	31.3	1.5	1.97
9	−1	−1	−1	+1	−1	39.9	37.6	1	0.97
10	+1	−−1	−1	+1	+1	124.9	117.8	2.3	2.6
11	−1	+1	−1	+1	+1	97.8	98.2	2.3	2.2
12	+1	+1	−1	+1	−1	25.6	34.8	1.8	1.97
13	−1	−1	+1	+1	+1	110	130.1	1.8	1.52
14	+1	−1	+1	+1	−1	91.8	109.96	2.3	2.05
15	−1	+1	+1	+1	−1	95	90.4	2	1.65
16	+1	+1	+1	+1	+1	160.8	127.3	2.4	2.52
17	0	0	0	0	0	96.2	82.23	2.2	1.94
18	0	0	0	0	0	95.8	82.23	2.3	1.94
19	0	0	0	0	0	95.7	82.23	2.2	1.94

Table 2. Experimental matrix for the 2^{5-1} FFD and responses for iron uptake and growth.

experiment's error. b_0 showed the constant coefficient, while b_i ($i = 1–5$) refers to the linear coefficient. b_{ij} ($i \neq j$) represents the second-order coefficient, and b_{ii} ($i = 1–4$) signifies the second-order interaction coefficient. The independent variables denoted by x. In the present study, the independent variables were coded as A, B, C, D, and E. Eventually, the predicted model was confirmed for variables used in current design.

Statistical analysis

The statistical analysis of the outcomes was conducted by Design Expert@ version 7.0.0. The qualities of fitted models assessed based on the coefficient of determination (R^2). To assess the significance of each term, the ANOVA combined with the F-test was employed to analyze the iron concentration in the cell plate and dry weight of biomass, with a significance level of $p \leq 0.05$. The location of the optimum variables was estimated using solving the fitted model.

Results and discussion

Biosynthesis of nanoparticles

As demonstrated in Fig. 1A (the FESEM image of the purified superparamagnetic Fe_3O_4 nanoparticles), biogenic magnetite nanoparticles well dispersed and spherical shape. The particle size distribution of biogenic magnetite nanoparticles based on the FESEM image is demonstrated in Fig. 1B. The particle size histogram of magnetite nanoparticles indicates that the particle size ranges from 10 to 110 nm which may be due to the magnetic property that they attach. The frequency distribution revealed that almost 50% of the particles are in the range of 10–40 nm.

Optimization of biogenic magnetite nanoparticles production

The first step towards optimization is to identify the components of the medium that have a notable effect on magnetite nanoparticles biosynthesized by strain ASFS1. Five medium components were evaluated at specified levels (Table. 1). The color change of the culture medium to a brownish-black hue after 96 h showed in 19 runs, which indicates the production of magnetite nanoparticles (Fig. 2). The Fe content in biomass and dried biomass results in an augmented 2^{5-1} FFD with the levels in coded units described in Table 2. The response range were from 25.6 to 160.8 μg mL^{-1} for Fe content in biomass (response 1) and 1.0–3.3 mg mL^{-1} for dried biomass (response 2). To the analysis of the response effects and assess the significance of the model terms, the ANOVA tables were designed (Table 3 for response 1 and response 2).

The normality of the data for both responses examined using plotting a normal probability plot of the residuals. According to Fig. 3, the data points on the plot fall fairly near to the straight line, which indicates the data follows a normal distribution with a relatively consistent variance throughout the responses range.

In response 1, X_4, X_5, X_1 X_2, X_3 X_4 are significant model terms. The p-value of Na_2-EDTA (X_4) was less than 0.05 (Table 3), thus this parameter had a significant effect on superparamagnetic Fe_3O_4 nanoparticles production strain ASFS1. Alphandéry et al[29]. reported addition of iron-chelating agents (specially EDTA) to the bacterial growth medium enables the enhance of the growth of *Magnetospirillum magneticum* strain AMB-1, an increase production yield of the magnetosomes size and chain length and yielded improved magnetosome heating properties. The kinetics of magnetosome synthesis in *Magnetospirillum magneticum* strain AMB-1 probably happens after the bacteria have reached the stationary phase[29,30]. Adding iron-chelating agents to the growth medium improves the rate of production of magnetic nanoparticles strain AMB-1[29]. Nevertheless, in the strain MSR-1, magnetosomes are produced before the bacteria have reached the stationary phase, possibly due to various mechanisms of magnetosome formation or iron uptake[29,31]. Thus, the effects of the presence of iron-chelating agents on the rate of magnetosome formation may be less noticeable for strain MSR-1 than strain AMB-1[29,31]. Therefore, EDTA as an iron-chelating factor has a positive effect on the growth and iron uptake in the strain ASFS1 of this study, similar to the AMB-1strain[29], due to probably the mechanism of formation of magnetic nanoparticles in both strains being similar and different from the MSR1 strain[31]. Similar to our study, Heyen et al[31]. and Alphandéry et al[29]. optimized the components of the culture medium for strains MSR-1 and AMB-1 respectively, unlike the present study, none of them used the experimental design method. The use of statistical methods such as Design Expert to design optimization experiments enhanced the efficiency and precision, and it provides investigation of several factors simultaneously. Finally, it improved the comprehensiveness of optimization results in bioprocessing applications[25]. Iron is a significant factor influencing the production of magnetic nanoparticles using magnetotactic bacteria[32,33]. Fe (III) deposited directly inside the bacterial cells comprising magnetosomes[32]. However, magnetotactic bacteria can utilize different iron sources, but the association between growth bacteria and iron uptake is not so clear[33]. Analysis of various concentrations of $FeCl_3$ (X_5) exhibited that this factor had considerable effect on magnetite nanoparticles production by strain ASFS1 ($p < 0.05$), while different concentration of $FeSO_4$ had not significant effects ($p < 0.05$). Similar to our study, kabary et al[33]. reported that $FeSO_4$ were less significant effects for bacterial growth and iron uptake by *Pseudomonas aeruginosa* Kb1 (confirmed as magnetotactic bacteria). Some studies have used $FeSO_4$ as a single source of iron[34,35]. Berny et al[22]. used $FeSO_4$ and $FeCl_3$ as iron sources for the production of magnetic nanoparticles by magnetotactic bacteria, similar to our study. Although, various concentrations of $FeSO_4$ had not significant effects, the interaction effect of X_3 X_4 is significant ($p < 0.05$) in the present study. Table 3 revealed that the yeast concentration (X_1) and tryptone concentration (X_2) not significant separately, while the interaction of X_1X_2 is significant. Yang et al[36]. showed yeast extract is not significant in magnetic nanoparticle production by bacteria. Their results are similar to our study, whereas peptone only improves the final bacterial cell density. Furthermore, adding only yeast extract and polypeptide as a culture medium produces a small number of magnetosomes[37], similar to the current study.

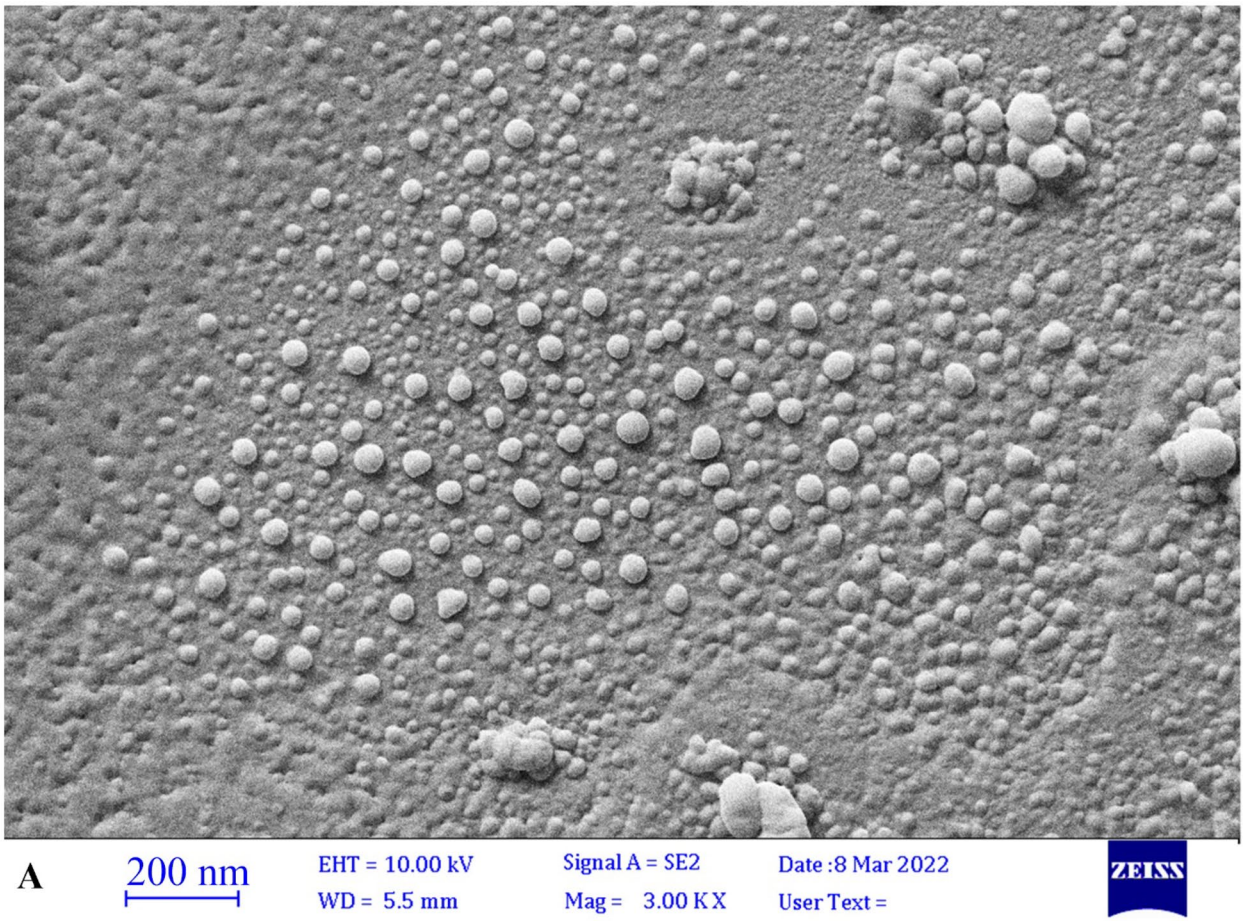

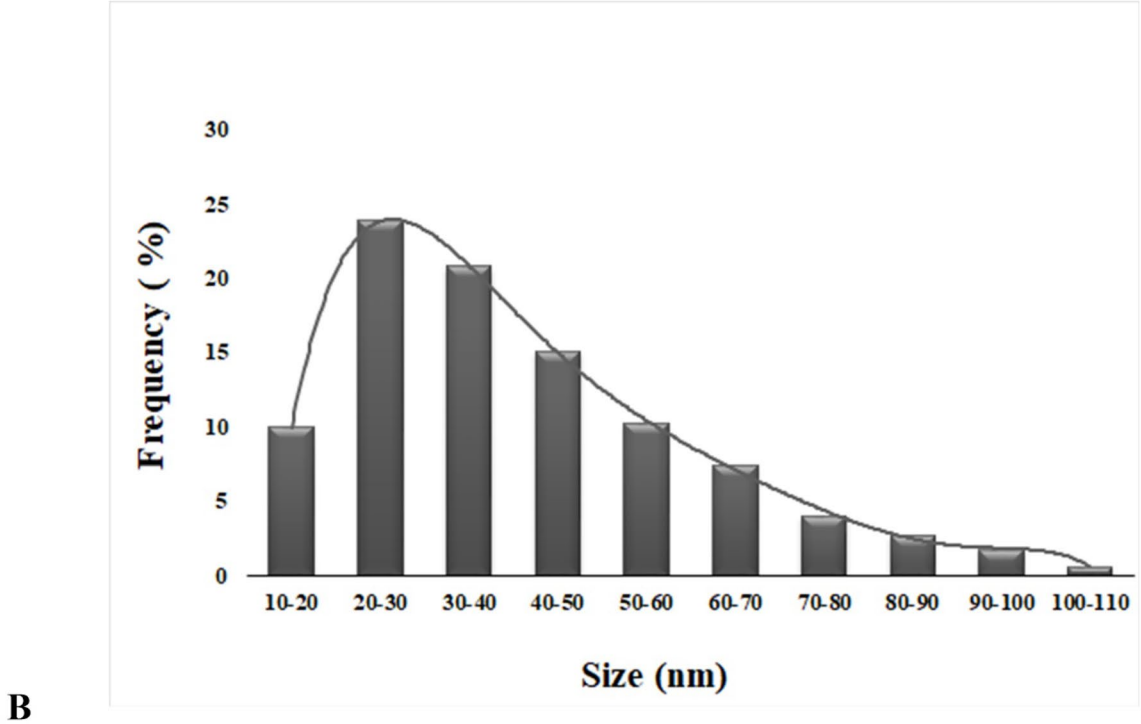

Fig.1. (**A**). FESEM image of Fe_3O_4 nanoparticles synthesized by strain ASFS1;(**B**). Particle size distribution of the biogenic magnetite nanoparticles obtained from FESEM images.

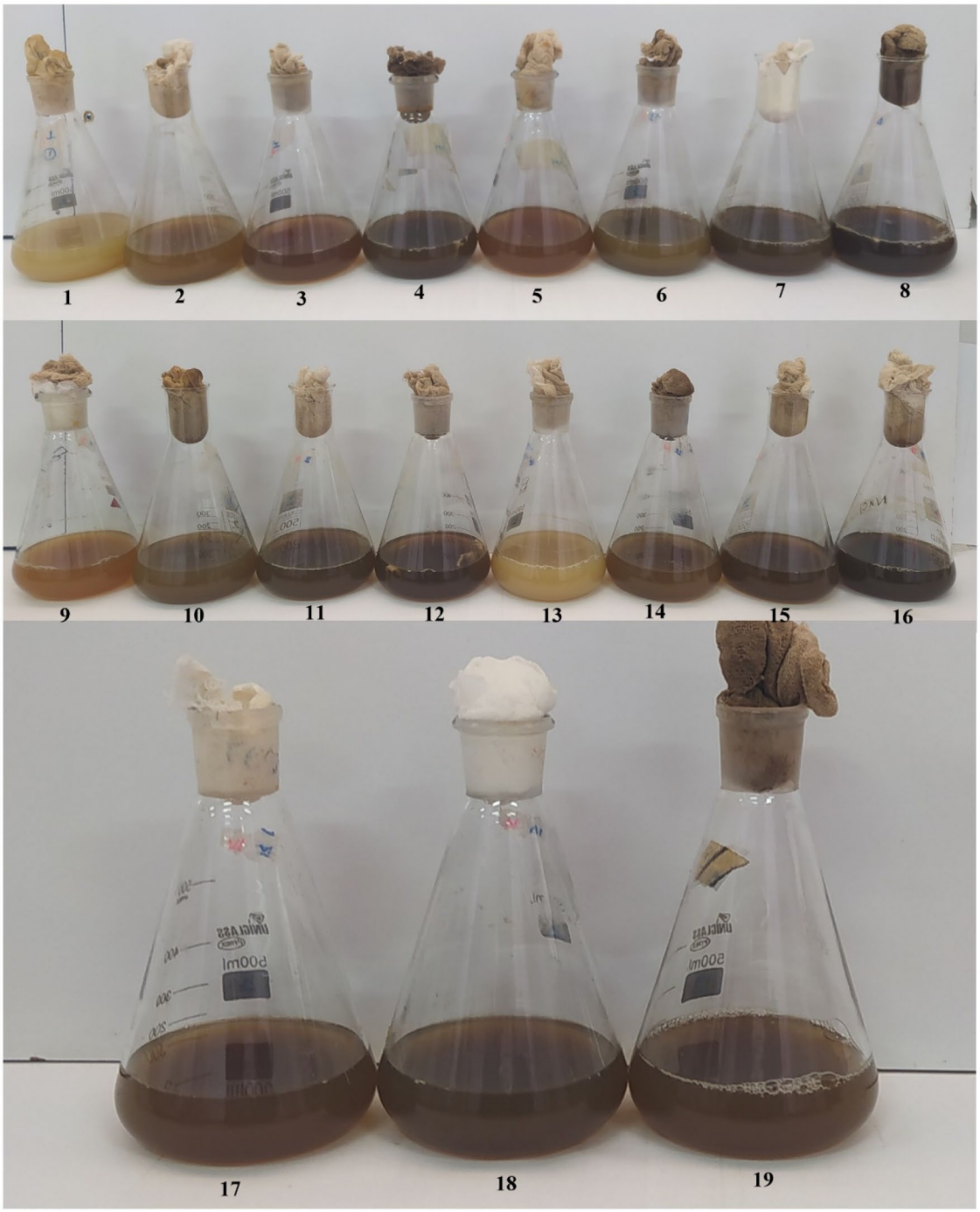

Fig. 2. Changing the color of the culture medium in 19 different runs designed with different components of the culture medium. The change in the color of the culture medium to brownish-black indicates an increase iron uptake by strain ASFS1. The result of increase for iron uptake by this strain is to increase the synthesis of magnetic nanoparticles. The result of increase for iron uptake by this strain is to increase the synthesis of magnetic nanoparticles.

Figure 4A, B exhibited one factor affecting Fe content in biomass within their experimental range while holding four factors constant. Furthermore, Fig. 4C, D illustrate the interaction of two factors, which the other three factors are kept constant. In Fig. 4A, tryptone (10 g L^{-1}), yeast extract (5 g L^{-1}), $FeSO_4$ (50 µg mL^{-1}), and $FeCl_3$ (100 µg mL^{-1}) are constant, and with increasing Na_2-EDTA concentration, the amount of iron in the biomass significantly increased. Analysis of response at the different levels of $FeCl_3$ when tryptone (10 g L^{-1}), yeast extract (5 g L^{-1}), $FeSO_4$ (50 µg mL^{-1}), and Na_2-EDTA (100 µg mL^{-1}) are constant, indicating that $FeCl_3$ considerably increased iron in the biomass (Fig. 4B). The interaction of tryptone and yeast extract on iron in the biomass (Fig. 4C) exhibited that by raising tryptone, the amount of iron in biomass not significantly raised, while using increasing yeast extract, the amount of iron in biomass considerably increased (constant factors:

Source of variation	Sum of square	df	Mean of square	F value	P > F
Model	18,317.44	7	2616.78	8.42	0.0016
X_1	280.56	1	280.56	0.90	0.3645
X_2	501.76	1	501.76	1.61	0.2327
X_3	1380.12	1	1380.12	4.44	0.0614
X_4	1958.06	1	1958.06	6.30	0.0309
X_5	10,070.12	1	10,070.12	32.39	0.0002
$X_1 X_2$	1870.56	1	1870.56	6.02	0.0341
$X_3 X_4$	2256.25	1	2256.25	7.26	0.0225
Curvature	472.44	1	472.44	1.52	0.2459
Residual	3108.97	10	310.90		
Lack of Fit	3108.83	8	388.60	5551.48	0.0002
Pure Error	0.14	2	0.070		
Cor Total	21,898.85	18			

Table 3. ANOVA for dependent variable: Fe content in biomass.

50 µg mL^{-1} of $FeSO_4$, 100 µg mL^{-1} of Na_2-EDTA and 100 µg mL^{-1} of $FeCl_3$). Thus, yeast extract alone has no effect on the amount of iron in biomass, but its interaction with tryptone has a significant effect on increasing the amount of iron in biomass. In Fig. 4D, the interaction of $FeSO_4$ and Na_2-EDTA shows that the amount of iron in biomass does not increase with the increase level of $FeSO_4$, while increase level of Na_2-EDTA lead to the amount of iron in biomass increases significantly).

In response 2, X_1, X_5, X_1 X_2 are significant model terms. The p-value of yeast extract (X_1) and $FeCl_3$ (X_5) was less than 0.05 (Table 4). Therefore, both parameters have significant effects on magnetite nanoparticles production strain ASFS1. Contrary to Yang et al[36]. study that polypeptone increases the biomass dry weight and yeast extract has no significant, the yeast extract increases biomass dry weight in the present study. Also, the interaction effects of yeast extract and tryptone (X_1X_2) is significant ($p < 0.05$).

Figure 5A, B displayed one factor affecting dried biomass within their testing range and keeping four factors' constants. In addition, Fig. 5C revealed the interaction of two factors, which the further three factors are held constant. The results show that increasing the level of yeast extract and $FeCl_3$ separately, has led to a significant increase in dry biomass (Fig. 5A, B, respectively). In Fig. 5C, the interaction of yeast extract and tryptone displays that dry biomass does not significantly rise with the raised level of tryptone, while the enhanced level of yeast extract leads to dry biomass enhancing considerably (constant factors: 100 µg mL^{-1} of $FeCl_3$, 100 µg mL^{-1} of Na_2-EDTA and 50 µg mL^{-1} of $FeSO_4$).

The fitted model (in the terms of coded values) for estimating Fe content in biomass (3) and dried biomass from 1 cc culture (4) by the selected strain were, respectively:

$$\begin{aligned}\text{Fe content in Biomassfrom 1 cc culture} = {} & +82.23 + 4.19X_1 - 5.60X_2 + 9.29X_3 \\ & + 11.06X_4 + 25.09X_5 - 10.81X_1X_2 + 11.88X_3X_4\end{aligned} \quad (3)$$

$$\text{Dried Biomass from 1 cc culture} = +1.94 + 0.35X_1 + 0.15X_2 + 0.28X_5 - 0.19X_1X_2 \quad (4)$$

The effects of X_1, X_3, X_4, X_5, *and* X_3 X_4 were positive (synergistic), while X_2 and X_1 X_2 had negative (antagonism) effects on Fe content in biomass. In response 2, the effects of X_1, X_2, X_5 were synergistic and only X_1 X_2 had antagonism effects on Dried Biomass.

The Model F-value of 8.42 and 8.57 for response 1 and response 2 respectively, implies the models are significant. Furthermore, values of "Prob > F" less than 0.0500 for both responses indicate model terms are significant. There is only a 0.16% and a 0.13% chance that a "Model F-value" this large could occur due to noise for responses 1 and 2, respectively. The relatively high value of $R^2 = 0.8549$ (response 1) and $R^2 = 0.7251$ (response 2) indicated that the models were significantly fitted. The higher the R^2 value (closer to the number one) indicates better the model fits, as it explains more of the data's variance. In this study, $R^2 = 0.8549$ (response 1) and $R^2 = 0.7251$ (response 2) indicate a good quality model that explains 85% and 72% of the data variance, respectively.

The location of optimum levels by the selected model for Fe content in biomass (158 µg mL^{-1}) and dried biomass (2.59 mg mL^{-1}) were predicted to be 7.95 g L^{-1} of yeast extract, 5 g L^{-1} of tryptone, 75 µg mL^{-1} of $FeSO_4$, 192.3 µg mL^{-1} of Na_2-EDTA and 150 µg mL^{-1} of $FeCl_3$.

To confirm the model adequacies for predicting Fe content in biomass and dried biomass, one additional experiment (repeated three times) by the same medium composition were performed. In the event that the average of the validation outcomes was within the limits of the confidence interval (CI), then the significant parameters and suitable levels for acquiring the desired outcomes were correctly selected[38]. The outcomes of three validation experiments demonstrated that there are good agreements between the predicted (The Fe content in biomass and dried biomass were 158 µg mL^{-1} and 2.59 mg mL^{-1}, respectively) and experimental (The Fe content in biomass and dried biomass were 139 ± 13 µg mL^{-1} and 2.2 ± 0.2 mg mL^{-1}, respectively) outcomes that revealed the chosen model was able to navigate within the design space.

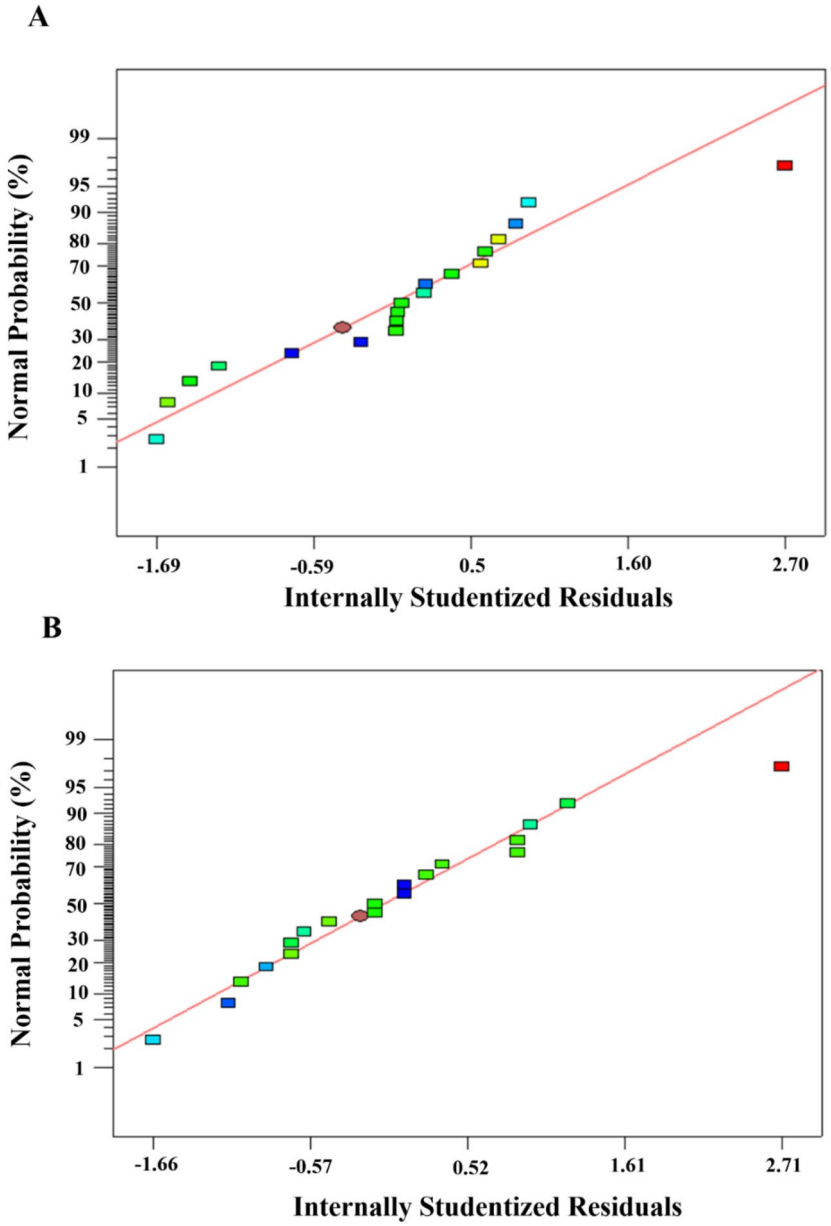

Fig. 3. The normal probability plot of the residuals, (**A**). for Response 1 and (**B**). for response 2.

Conclusion

The present study was aimed to optimize culture media components for strain ASFS1 growth and magnetite nanoparticles formation by fractional factorial designs. Yeast extract, tryptone, and $FeSO_4$ were confirmed not to be very significant factors considering to Fe content in biomass assisted by strain ASFS1, while Na_2-EDTA, $FeCl_3$, interaction yeast extract-tryptone, and interaction $FeSO_4$- Na_2-EDTA were illustrated the significant effect on Fe content in biomass. Tryptone was proved not significant parameter considering to dried biomass, while yeast extract, $FeCl_3$, and interaction yeast extract-tryptone were demonstrated a significant effect on dried biomass of strain ASFS1. In both responses 1 and 2, the factors of $FeCl_3$ and interaction effects yeast extract-tryptone are significant ($p < 0.05$). The maximum fe content in biomass, along with the maximum dried biomass, were achieved at 7.95 g L^{-1} of yeast extract, 5 g L^{-1} of tryptone, 75 µg mL^{-1} of $FeSO_4$, 192.3 µg mL^{-1} of Na_2-EDTA and 150 µg mL^{-1} of $FeCl_3$. Nevertheless, further studies must be accomplished to find about the related pathway involved in magnetite nanoparticles biosynthesis and the potential application of this strain for large-scale production of superparamagnetic Fe_3O_4 nanoparticles.

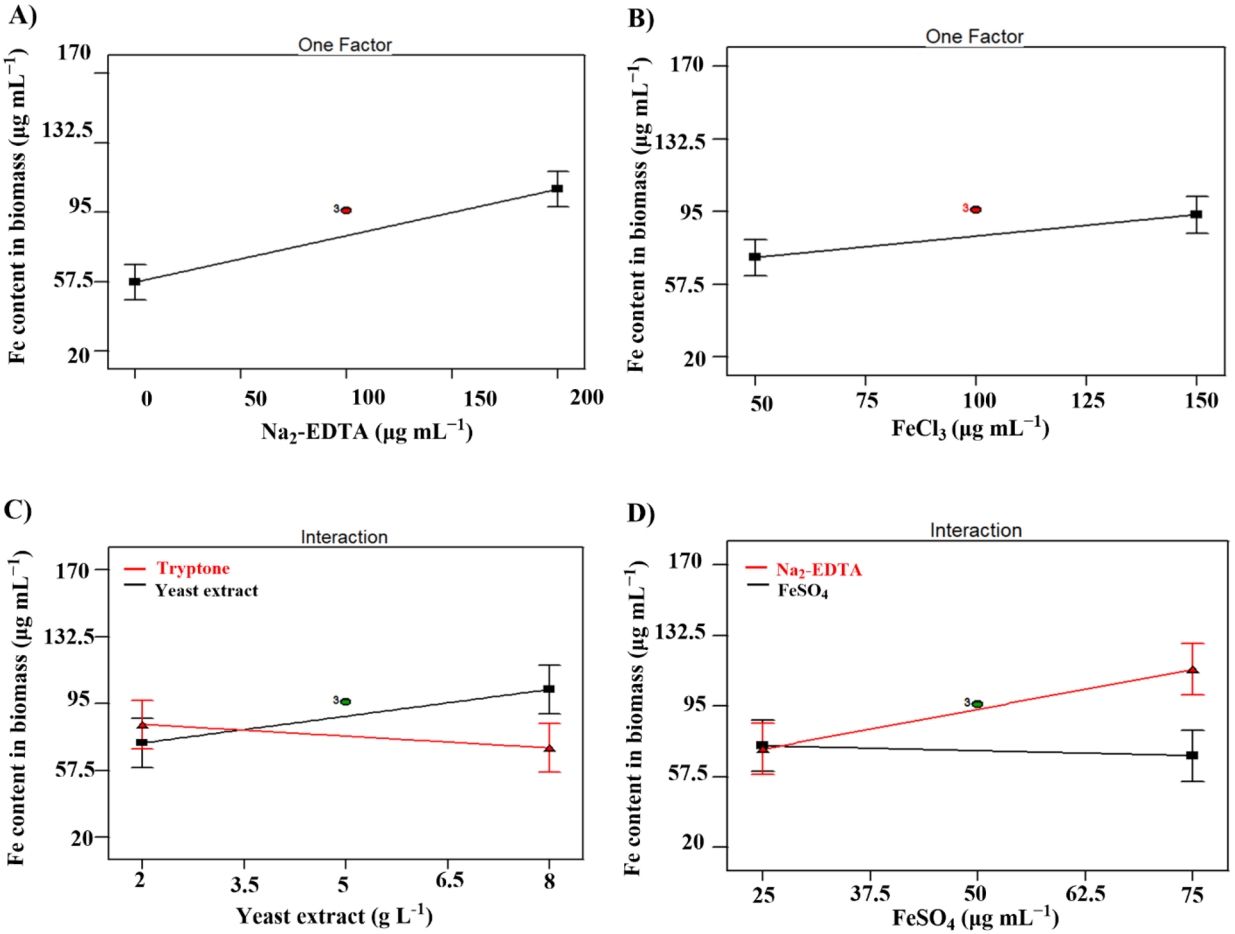

Fig. 4. Interaction plot within the ANOVA for factors affecting on Fe content in biomass (of 1 cc culture medium); **A**) Na_2-EDTA, **B**) $FeCl_3$, **C**) Tryptone- yeast extract interaction and **D**) Na_2-EDTA and $FeSO_4$ interaction.

Source of variation	Sum of square	df	Mean of square	F value	P > F
Model	4.09	4	1.02	8.57	0.0013
X_1	1.96	1	1.96	16.42	0.0014
X_2	0.36	1	0.36	3.02	0.1061
X_5	1.21	1	1.21	10.14	0.0072
$X_1 X_2$	0.56	1	0.56	4.71	0.0490
Curvature	0.22	1	0.22	1.85	0.1966
Residual	1.55	13	0.12		
Lack of Fit	1.54	11	0.14	42.14	0.0234
Pure Error	6.667E-003	2	3.333E-003		
Cor Total	5.87	18			

Table 4. ANOVA for dependent variable: dried biomass.

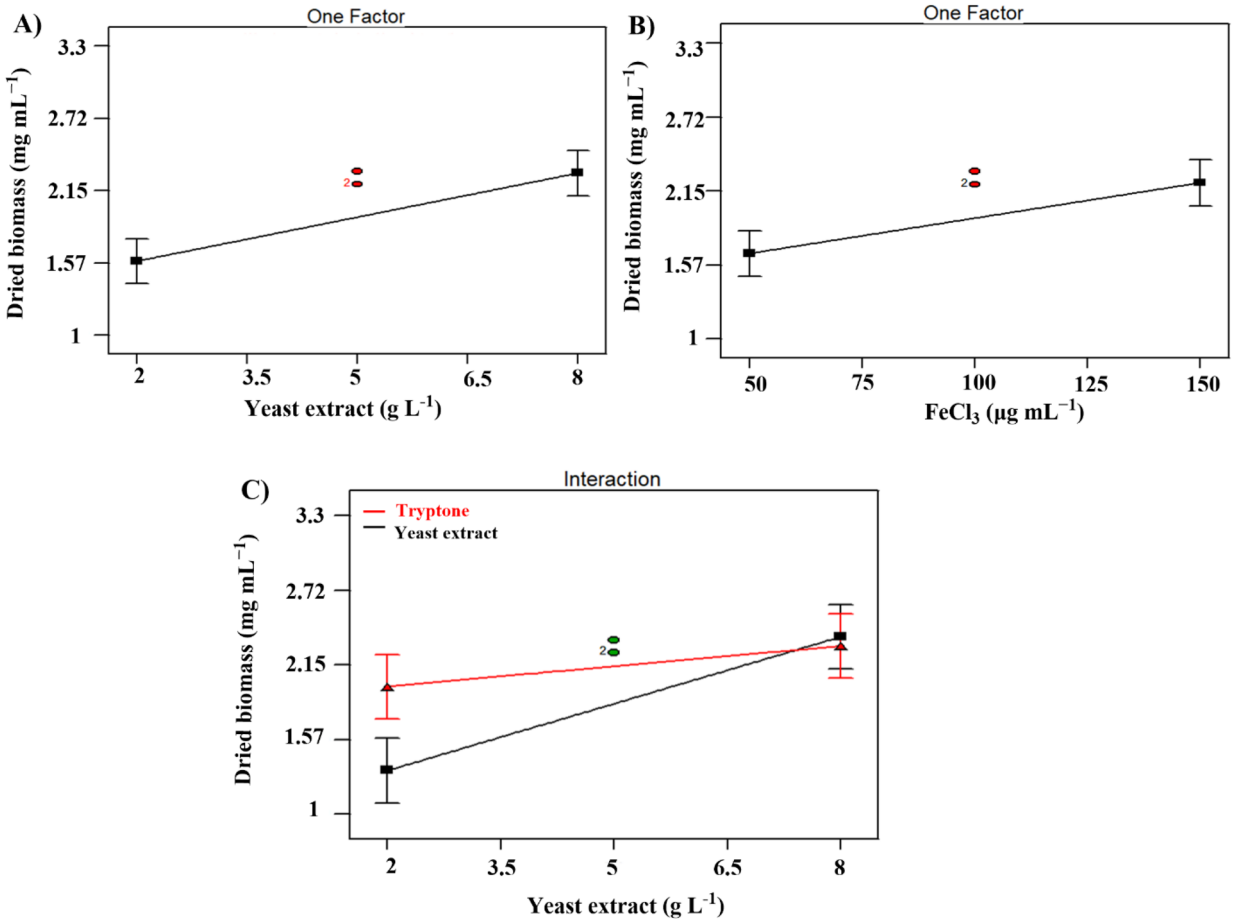

Fig. 5. Interaction plot within the ANOVA for factors affecting on dried biomass (of 1 cc culture medium); **A**) yeast extract **B**) $FeCl_3$ and **C**) Tryptone- yeast extract interaction.

Data availability

All data generated or analyzed during current study included in this manuscript.

Received: 8 March 2024; Accepted: 22 August 2024
Published online: 29 August 2024

References

1. Kirya, P. *et al.* Biomimicry of Blue Morpho butterfly wings: An introduction to nanotechnology through an interdisciplinary science education module. *J. Soc. Inform. Disp.* **29**, 896–915 (2021).
2. Satarzadeh, N. *et al.* Facile microwave-assisted biosynthesis of arsenic nanoparticles and evaluation their antioxidant properties and cytotoxic effects: a preliminary in vitro study. *J. Clust. Sci.* **34**(4), 1831–1839 (2022).
3. Satarzadeh, N. *et al.* An insight into biofabrication of selenium nanostructures and their biomedical application. *3 Biotech* **13**, 79 (2023).
4. Abdullah, N. H. Optimization of magnetic nano-iron production by Aspergillus flavipes MN956655. 1 using response surface methodology and evaluation of their dye decolorizing and antifungal activities. *Sci. Rep.* **12**, 21059 (2022).
5. Khan, I., Saeed, K. & Khan, I. Nanoparticles: Properties, applications and toxicities. *Arab. J. Chem.* **12**, 908–931 (2019).
6. Nguyen, M. D., Tran, H.-V., Xu, S. & Lee, T. R. J. A. S. Fe_3O_4 nanoparticles: Structures, synthesis, magnetic properties, surface functionalization, and emerging applications. *Appl. Sci.* **11**, 11301 (2021).
7. Singamaneni, S., Bliznyuk, V. N., Binek, C. & Tsymbal, E. Y. Magnetic nanoparticles: recent advances in synthesis, self-assembly and applications. *J. Mater. Chem.* **21**, 16819–16845 (2011).
8. Lisjak, D. & Mertelj, A. Anisotropic magnetic nanoparticles: A review of their properties, syntheses and potential applications. *Progr. Mater. Sci.* **95**, 286–328 (2018).
9. Koh, I. & Josephson, L. Magnetic nanoparticle sensors. *Sensors* **9**, 8130–8145 (2009).
10. Chen, Y.-T., Kolhatkar, A. G., Zenasni, O., Xu, S. & Lee, T. R. J. S. Biosensing using magnetic particle detection techniques. *Sensors* **17**, 2300 (2017).
11. Bilal, M., Zhao, Y., Rasheed, T. & Iqbal, H. M. N. Magnetic nanoparticles as versatile carriers for enzymes immobilization: A review. *Int. J. Biol. Macromol.* **120**, 2530–2544 (2018).
12. Wu, K. *et al.* Magnetic-nanosensor-based virus and pathogen detection strategies before and during COVID-19. *ACS Appl. Nano Mater.* **3**, 9560–9580 (2020).
13. Laurent, S. *et al.* Magnetic iron oxide nanoparticles: Synthesis, stabilization, vectorization, physicochemical characterizations, and biological applications. *Chem. Rev.* **108**, 2064–2110 (2008).

14. Ling, D. & Hyeon, T. J. S. Chemical design of biocompatible iron oxide nanoparticles for medical applications. *Small* **9**, 1450–1466 (2013).
15. Bobo, D., Robinson, K. J., Islam, J., Thurecht, K. J. & Corrie, S. R. Nanoparticle-based medicines: a review of FDA-approved materials and clinical trials to date. *Pharmaceut. Res.* **33**, 2373–2387 (2016).
16. Teja, A. S. & Koh, P.-Y. Synthesis, properties, and applications of magnetic iron oxide nanoparticles. *Prog. Cryst. Growth Charact. Mater.* **55**, 22–45 (2009).
17. Kuppusamy, P., Yusoff, M. M., Maniam, G. P. & Govindan, N. Biosynthesis of metallic nanoparticles using plant derivatives and their new avenues in pharmacological applications–an updated report. *Saudi Pharmaceut. J.* **24**, 473–484 (2016).
18. Bhardwaj, B., Singh, P., Kumar, A., Kumar, S. & Budhwar, V. J. A. P. B. Eco-friendly greener synthesis of nanoparticles. *Adv. Pharmaceut. Bull.* **10**, 566 (2020).
19. Ahmed, S. F. *et al.* Green approaches in synthesising nanomaterials for environmental nanobioremediation: Technological advancements, applications, benefits and challenges. *Environ. Res.* **204**, 111967 (2022).
20. Singh, P., Kim, Y.-J., Zhang, D. & Yang, D.-C. Biological synthesis of nanoparticles from plants and microorganisms. *Trends Biotechnol.* **34**, 588–599 (2016).
21. Rana, A., Yadav, K. & Jagadevan, S. A comprehensive review on green synthesis of nature-inspired metal nanoparticles: Mechanism, application and toxicity. *J. Clean. Prod.* **272**, 122880 (2020).
22. Berny, C. *et al.* A method for producing highly pure magnetosomes in large quantity for medical applications using *Magnetospirillum* gryphiswaldense MSR-1 magnetotactic bacteria amplified in minimal growth media. *Front. Bioeng. Biotechnol.* **8**, 16 (2020).
23. Moon, S., Saboe, A. & Smanski, M. J. Using design of experiments to guide genetic optimization of engineered metabolic pathways. *J. Ind. Microbiol. Biotechnol.* **51**, 010 (2024).
24. Khaw, K.-Y. *et al.* Factorial design-assisted supercritical carbon-dioxide extraction of cytotoxic active principles from Carica papaya leaf juice. *Sci. Rep.* **9**, 1716 (2019).
25. Weissman, S. A. & Anderson, N. G. Design of experiments (DoE) and process optimization. A review of recent publications. *Org. Process Res. Dev.* **19**, 1605–1633 (2015).
26. Jankovic, A., Chaudhary, G. & Goia, F. Designing the design of experiments (DOE)–An investigation on the influence of different factorial designs on the characterization of complex systems. *Energy Build.* **250**, 111298 (2021).
27. Satarzadeh, N., Shakibaie, M., Forootanfar, H. & Amirheidari, B. Purification, characterization, and assessment of anticancer activity of iron oxide nanoparticles biosynthesized by novel thermophilic *Bacillus tequilensis* ASFS1. *J. Basic Microbiol.* https://doi.org/10.1002/jobm.202400153 (2024).
28. Rosenfeldt, S. *et al.* Towards standardized purification of bacterial magnetic nanoparticles for future in vivo applications. *Acta Biomater.* **120**, 293–303 (2021).
29. Alphandéry, E., Amor, M., Guyot, F. & Chebbi, I. The effect of iron-chelating agents on *Magnetospirillum* magneticum strain AMB-1: Stimulated growth and magnetosome production and improved magnetosome heating properties. *Appl. Microbiol. Biotechnol.* **96**, 663–670. https://doi.org/10.1007/s00253-012-4199-5 (2012).
30. Yang, C.-D. *et al.* Synthesis of bacterial magnetic particles during cell cycle of *Magnetospirillum* magneticum AMB-1. *Appl. Biochem. Biotechnol.* **91**, 155–160 (2001).
31. Heyen, U. & Schüler, D. Growth and magnetosome formation by microaerophilic Magnetospirillum strains in an oxygen-controlled fermentor. *Appl. Microbiol. Biotechnol.* **61**, 536–544 (2003).
32. Moisescu, C., Bonneville, S., Staniland, S., Ardelean, I. & Benning, L. G. Iron uptake kinetics and magnetosome formation by *Magnetospirillum* gryphiswaldense as a function of pH, temperature and dissolved iron availability. *Geomicrobiol. J.* **28**, 590–600 (2011).
33. Kabary, H., Eida, M. F., Attia, M., Awad, N. & Easa, S. M. Optimization of growth and Fe uptake by *Pseudomonas aeruginosa* Kb1 for biosynthesis of magnetic nanoparticles. *Middle East J.* **7**, 1503–1513 (2018).
34. Yan, L. *et al.* Optimization of magnetosome production by *Acidithiobacillus* ferrooxidans using desirability function approach. *Mater. Sci. Eng. C* **59**, 731–739 (2016).
35. Zhang, S., Yan, L., Li, H. & Liu, H. J. Optimal conditions for growth and magnetosome formation of *Acidithiobacillus* ferrooxidans. *Afr. J. Microbiol. Res.* **6**, 6142–6151 (2012).
36. Yang, C.-D., Takeyama, H., Tanaka, T., Matsunaga, T. J. E. & Technology, M. Effects of growth medium composition, iron sources and atmospheric oxygen concentrations on production of luciferase-bacterial magnetic particle complex by a recombinant Magnetospirillum magneticum AMB-1. *Enzyme Microb. Technol.* **29**, 13–19 (2001).
37. Basit, A., Wang, J., Guo, F., Niu, W. & Jiang, W. Improved methods for mass production of magnetosomes and applications: A review. *Microb. Cell Fact.* **19**, 1–11 (2001).
38. Anderson, M. J. & Whitcomb, P. J. *DOE simplified: practical tools for effective experimentation* (CRC Press, 2017).

Acknowledgements

The present study was financially supported using grant NO: BIODC-34975-35555.2 and 99000469 of the Biotechnology Development Council of the Islamic Republic of Iran and Faculty of Pharmacy, Kerman University of Medical Sciences, Kerman, Iran, respectively.

Author contributions

N.S. Methodology, Validation, Investigation, Resources, Writing—Original Draft, Writing—Review & Editing. B.A. Methodology, Data Curation, Resources, Writing—Review & Editing, Supervision, Project administration. M.Sh. Methodology, Validation, Formal analysis, Writing—Review & Editing, Supervision, Project administration. H.F. Methodology, Writing—Review & Editing, Supervision.

Competing interests

The authors declare no competing interests.

Additional information

Correspondence and requests for materials should be addressed to B.A. or M.S.